Chapter 5

SENSITIVITY

5.1 Introduction

This chapter analyses the noise sources in the zero-field electron spin resonance spectrometer. These considerations are very important because, as will be discussed in Chapter 6, the width of the atomic resonance and the sensitivity of the atomic resonance measurement determine the short-term stability of a passive atomic frequency standard. The three basic components of the spectrometer which contribute to random instabilities are (Figure 5.1): (1) frequency fluctuations and tuning voltage noise of the loop-gap resonator, (2) phase noise of the voltage-controlled oscillator, and (3) the noise floor of the mixer or receiver. In addition, technical sources of background interference include acoustic pickup by the loop-gap resonator, magnetic pickup of the audio modulation field, and spurs on the RF carrier from 60 Hz pickup. The following three sections will analyze the random and technical noise sources of each of the basic components, along with possible improvements to the prototype design.

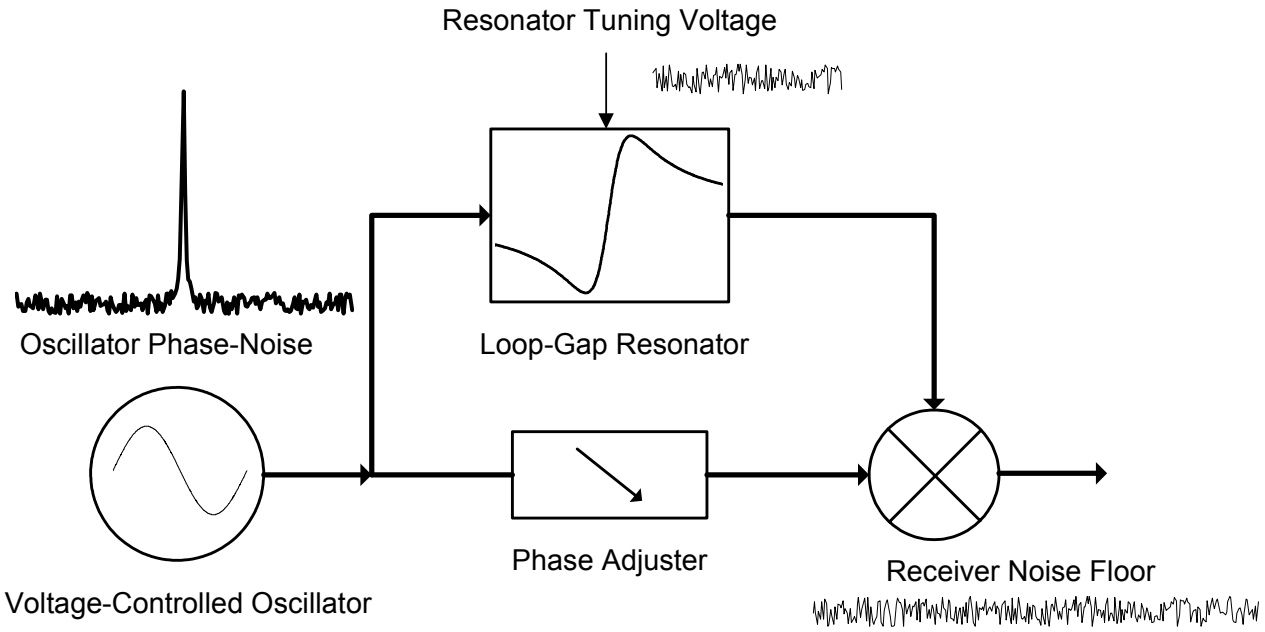

Figure 5.1: Noise Sources in the Frequency Discriminator

5.2 Resonator Noise

The loop-gap resonator is tuned using a piezo adjuster to control the capacitive gap. Noise from the piezo driver modulates the resonant frequency. Similarly, common-mode pick-up of the magnetic field modulation causes a spurious background at the spectrometer output.

In the ideal case, the two pieces of the loop-gap resonator are parallel, and therefore, the capacitive gap has a uniform spacing, as shown in Figure 5.2:

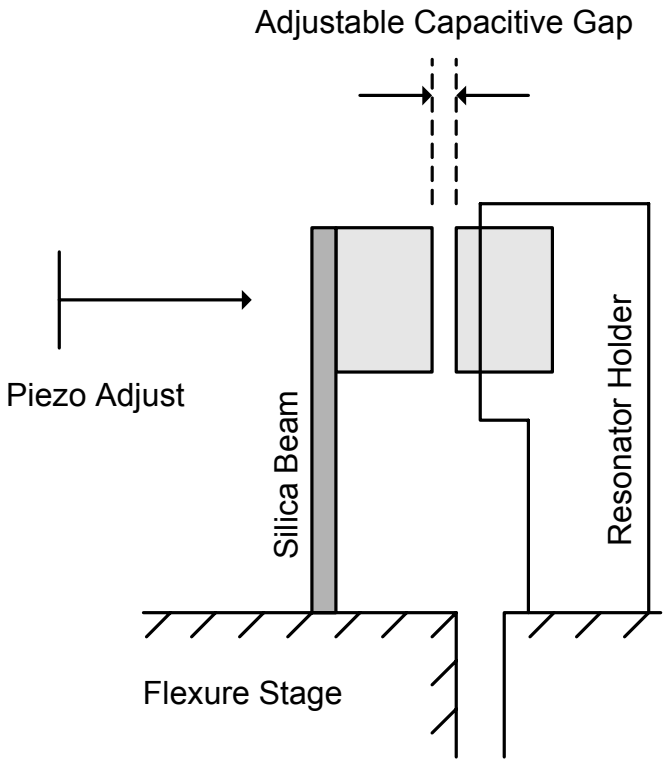

Figure 5.2: Tunable Loop-Gap Resonator Side View

The resonator is tuned using the piezo adjuster, which controls the approach of the capacitive gap. In the prototype, this gap is between 10 microns and 25 microns, and consequently the alignment of the resonator critical. In practice, the two resonator pieces are not perfectly aligned and at some lower frequency the resonator will short.

A 150 V piezo driver is used to adjust the resonator gap and therefore the tuning. Noise from the driver causes a random modulation of the resonator gap, and therefore random frequency modulation of the resonator, which adds to the spectrometer noise floor. One method to analyze the contribution is to measure the resonator frequency as a function of piezo voltage. The prototype loop-gap resonator tunes from ~ 1050 MHz @ 150 V to 1250 MHz @ 0V, with a mean slope of approximately 1.3 MHz / V.

The signal which results at the output of the frequency discriminator from noise on the piezo driver is as follows.

First, analyze the result of a small sinusoidal voltage on the piezo electrodes:

$$\Delta V = v \cdot \sin(\omega_m t) \tag{5.1}$$

The loop-gap resonator is frequency modulated

$$\Delta f = K \cdot v \cdot \sin(\omega_m t) \tag{5.2}$$

In the equation, K is the slope of the frequency tuning curve in MHz/V. The resulting phase modulation of the signal coupled through the resonator is:

$$\Delta\theta \cong \frac{2Q_L}{f_0} \cdot K \cdot v \cdot \sin(\omega_m t) \tag{5.3}$$

In the equation, f_0 is the center frequency of the resonator (MHz) and Q_L is the loaded-Q of the coupled resonator. In Figure 5.1, the mixer inputs are adjusted in quadrature to implement a phase detector, and assuming 6dB conversion loss:

$$\Delta V_M = \frac{1}{2} \cdot V_{RF} \cdot \sin\theta \cong \frac{1}{2} \cdot V_{RF} \cdot \Delta\theta = V_{RF} \cdot \frac{Q_L}{f_0} \cdot K \cdot v \cdot \sin(\omega_m t) \tag{5.4}$$

Therefore, *noise with a white noise spectrum from the piezo driver results in a white noise floor at the frequency discriminator output*, with a transfer function:

$$\left| \frac{V_{out}}{V_{piezo}} \right| = V_{RF} \frac{Q_L K}{f_0} \tag{5.5}$$

For example, assuming the carrier power at the RF port of the mixer is 0dBm, the resonator loaded-Q is ~400, the measurement frequency is 1100 MHz, and the sensitivity of the resonator tuning voltage is of 1.3 MHz/V, the transfer function Equation 5.5 is 0.15. Noise

on the piezo driver equal to $6nV/\sqrt{Hz}$ results in $0.9nV/\sqrt{Hz}$ at baseband, *i.e.*, is equivalent to the thermal noise of a 50 Ohm resistor at 300K.

A large electrolytic capacitor on the output of the piezo driver is an effective noise filter in combination with the 50 Ohm output impedance of the driver. This capacitor limits the bandwidth of the automatic frequency control loop used to maintain tracking between the local oscillator frequency and resonator center frequency. Noise and spurs from the piezo driver pose a problem if a faster loop is required.

A second consideration, which is very significant in the prototype design, is the sensitivity of the tunable resonator to vibrations and acoustics. Referring to Figure 5.2, vibrations of the flexure stage platform cause motion of the cantilevered beam holding one piece of the loop gap resonator. Sound waves also excite the beam. The combination of high-Q and a small capacitive gap means the resonator is very sensitive to these mechanical sources of noise.

Vibrations and Acoustics

The mechanically tuned loop-gap resonator used in the prototype is sensitive to vibrations and acoustics because of the very close spacing of the capacitor electrodes (~ 10 microns) and a mechanical design which uses a cantilevered beam from the flexure stage. The resonant frequency is given by:

$$(f_0)^2 = \frac{1}{(2\pi)^2 LC} = \frac{g}{(2\pi)^2 L\varepsilon_0 A} \tag{5.6}$$

and variations in the resonator frequency with the capacitance gap g are:

$$\frac{\Delta f_0}{f_0} = \frac{1}{2} \cdot \frac{\Delta g}{g} \tag{5.7}$$

The frequency deviation cause by mechanical vibration results in a phase variation of the carrier and therefore a voltage at the frequency-discriminator output:

$$\Delta V_M \cong \frac{1}{2} \cdot V_{RF} \cdot \Delta\theta = \frac{1}{2} V_{RF} \cdot \frac{Q_L}{f_0} \cdot \frac{1}{2} \frac{\Delta g}{g} f_0 \tag{5.8}$$

In practice, the largest vibration interference is below 500 Hz, which depends on the mechanical resonances of the loaded beam used to position the resonator (Figure 5.2). Choosing a magnetic field modulation frequency above 500 Hz is essential to avoid this interference. Any excessive vibration saturates the receiver chain.

Modulation Coil Acoustics

The Lorentz force between the modulation coils and windings generates sound and vibrations:

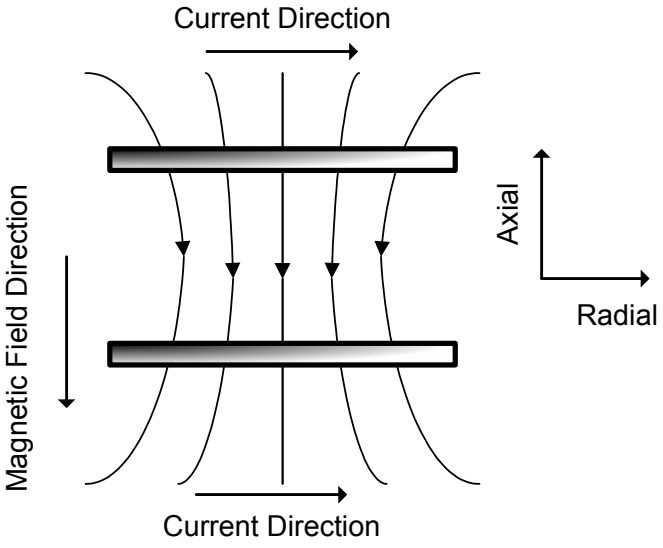

Figure 5.3 Lorentz Force Between Helmholtz Coils

Depending on the angle of fringing of the magnetic field at the modulation coils, there is a net force directed along the axis of the coil pair. There is no net force in the radial direction for circular symmetry. The Lorentz force is proportional to the square of the current, and therefore *the vibrations or acoustics of the modulation coils generate acoustics at the second harmonic of the bidirectional modulation waveform*. This signal is not rejected by the modulation waveform scheme discussed in Chapter 4 (Figure 4.3). A typical example of the measured background signal is shown below:

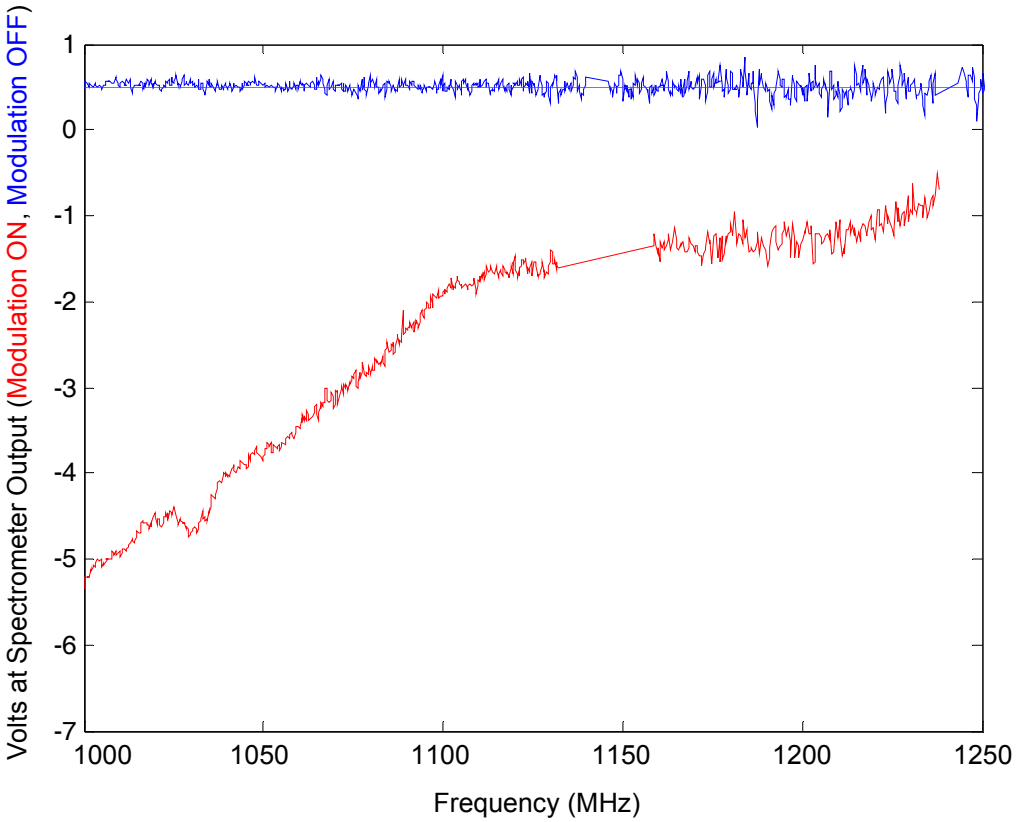

Figure 5.4 Background Pickup Signal During Spectrometer Sweep

Notice that the sensitivity to pickup increases at lower frequencies because the capacitive gap *g* is smaller, as in Equation 5.8. An improved tunable resonator design would take into account the problem with acoustic pickup. The current design, which uses a cantilevered beam for positioning the resonator, is especially sensitive to acoustics.

5.3 Receiver Noise Figure

Thermal noise is the only fundamental noise source in the frequency discriminator (Figure 5.1), provided the amplitude and phase noise of the carrier can be adequately reduced. The prototype design is far from optimal, in that no low-noise amplifier is used ahead of the mixer, and a 6 dB attenuator is used to match the mixer input port, with an equivalent loss

of power. In a refined design, however, thermal noise would be the limiting noise source. Carrier-suppression techniques may also be used to reduce noise from the source to below the receiver noise floor [1,2,3]. Another consideration is 1/f noise of the low-noise amplifier and mixer at high carrier powers, which has been studied for precision frequency discriminators [4].

5.4 Oscillator Phase Noise

This section analyzes the contributions of phase and amplitude noise of the oscillator to the measurement noise floor. While amplitude noise is shown to be a second-order effect when a frequency discriminator is used for measuring magnetic resonance, the phase noise of the oscillator is often the dominant random noise source in the spectrometer or frequency standard.

Techniques for reducing the close-in phase noise of a voltage-controlled oscillator are well known [3]. In particular, a second frequency discriminator may be used to measure and suppress (using feedback) the oscillator phase noise. The prototype oscillator uses a simple voltage-controlled LC oscillator. A coaxial resonator oscillator could have up to 20 dB better phase noise.

Phase Noise

Consider a phase modulated carrier:

$$V(t) = V\cos[2\pi f_c t + \beta\sin(2\pi f_m t)] \tag{5.9}$$

Assuming $\beta << 1$ this phase modulated signal is approximately equal to:

$$V(t) \cong V\cos(2\pi f_c t) - \beta V\sin(2\pi f_m t)\sin(2\pi f_c t) \tag{5.10}$$

$$V(t) \cong V\cos(2\pi f_c t) - \frac{\beta V}{2}\left[\cos(2\pi f_c t - 2\pi f_m t) - \cos(2\pi f_c t + 2\pi f_m t)\right] \tag{5.11}$$

The resonator dispersion introduces delay to the modulation sidebands equal to:

$$\Delta\theta_m = \pm\frac{2Q_L f_m}{f_0} \tag{5.12}$$

and therefore the signal couple coupled through the resonator is

$$V(t) \cong V\cos(2\pi f_c t) - \frac{\beta V}{2}\left[\cos(2\pi f_c t - 2\pi f_m t - \Delta\theta_m) - \cos(2\pi f_c t + 2\pi f_m t + \Delta\theta_m)\right] \tag{5.13}$$

The mixer output is:

$$V(t) \cong \left[V\cos(2\pi f_c t) - \frac{\beta V}{2}\left[\cos(2\pi f_c t - 2\pi f_m t - \Delta\theta_m) - \cos(2\pi f_m t + 2\pi f_m t + \Delta\theta_m)\right]\right]\cdot\left[V\sin(2\pi f_c t) + \beta V\sin(2\pi f_m t)\cos(2\pi f_c t)\right] \tag{5.14}$$

$$V(t) \cong V^2[\beta\sin(2\pi f_m t)\cdot\cos^2(2\pi f_c t) - \frac{\beta}{2}\left[\cos(2\pi f_c t - 2\pi f_m t - \Delta\theta_m) - \cos(2\pi f_m t + 2\pi f_m t + \Delta\theta_m)\right]\cdot\sin(2\pi f_c t)] \tag{5.15}$$

$$V(t) \cong V^2\beta[\sin(2\pi f_m t)\cdot\frac{1}{2} - \frac{1}{4}[\sin(2\pi f_m t + \Delta\theta) + \sin(2\pi f_m t + \Delta\theta)]] \tag{5.16}$$

$$V(t) \cong V^2\frac{\beta}{2}[\sin(2\pi f_m t) - \sin(2\pi f_m t + \Delta\theta)] \cong V^2\frac{\beta}{2}\Delta\theta\cos(2\pi f_m t) \cong V^2\frac{\beta}{2}\cdot\frac{2Q_L f_m}{f_0}\cos(2\pi f_m t) \tag{5.17}$$

The single-sideband power of the phase modulation is:

$$P_{FM,NB,SSB} = \frac{1}{2}\beta^2 \tag{5.18}$$

which results in a modulated signal power at the frequency discriminator output:

$$P_{PN,SSB} = \frac{1}{2}\beta^2\left(\frac{Q_L f_m}{f_0}\right)^2 \tag{5.19}$$

Hence, the transfer function between the phase-noise sideband power and the baseband noise floor is:

$$\frac{P_{out}}{P_{PhaseNoise}} = \left(\frac{Q_L f_m}{f_0}\right)^2 \tag{5.20}$$

In the above, f_m is the offset from carrier. Equation 5.20 shows that the $1/f^2$ phase noise region of the source generates a white noise power spectrum at baseband, and the $1/f^3$ phase noise region is demodulated to 1/f noise.

If the RF carrier power is 0dBm and the phase noise is -80dBc/Hz at 3.3 kHz offset (see Chapter 4.7), then the noise power at baseband is:

$$P = \left(\frac{400 * 3.3kHz}{1100MHz}\right)^2 - 80dBm = -138dBm \tag{5.21}$$

The noise power is equivalent to $27nV/\sqrt{Hz}$ at 50 Ohms. The phase noise may easily dominate the noise floor of the spectrometer.

Amplitude Noise

The amplitude noise of the oscillator is a second-order effect, as will be shown below. This "nulling" of the carrier amplitude noise is one reason for using the frequency discriminator design. Consider a sinusoidally amplitude modulated carrier:

$$V(t) = V\cos\omega_m t\cos\omega_c t = \frac{1}{2}V[\cos(\omega_m - \omega_c)t + \cos(\omega_m + \omega_c)t] \tag{5.22}$$

The response of the loop-gap resonator is:

$$\frac{V_o}{V_i} = \frac{2s/RC}{s^2 + 2s/RC + 1/LC} \tag{5.23}$$

$$\frac{V_o}{V_i} = \frac{2j\omega/RC}{\omega_0^2 - \omega^2 + 2j\omega/RC} \tag{5.24}$$

$$\frac{V_o}{V_i} = \frac{2j(\omega_0 + \omega_m)/RC}{\omega_0^2 - (\omega_0 + \omega_m)^2 + 2j(\omega_0 + \omega_m)/RC} \cong \frac{2j\omega_0/RC}{-2\omega_0\omega_m + 2j\omega_0/RC} = \frac{j/RC}{-\omega_m + j/RC} \tag{5.25}$$

The approximation is valid to the order of the ratio of the modulation frequency to the carrier frequency. For example, if the modulation frequency is 10 kHz and the carrier frequency is 1 GHz, the ratio is 10^{-5}. The approximation is extremely accurate up to modulation frequencies of 1 MHz (~ 0.1%).

The phase shift of the AM modulation sidebands is:

$$\theta = \frac{\pi}{2} - \tan^{-1}(1/\omega_m RC) \tag{5.26}$$

or in terms of loaded-Q:

$$\theta = \frac{\pi}{2} - \tan^{-1}(f_0/2Q_L\Delta f) \tag{5.27}$$

The dispersion at the resonator center frequency is:

$$\left.\frac{\partial\theta}{\partial\Delta f}\right|_{\Delta f=0} = \frac{2Q_L}{f_0} \tag{5.28}$$

and the approximate phase shift of the modulation sidebands is:

$$\Delta\theta_m = \pm\frac{2Q_L f_m}{f_0} \tag{5.29}$$

If the mixer is driven in quadrature, and assuming 6dB conversion loss, the mixer output is:

$$V_B(t) = \frac{1}{2}V\left[\cos\left((\omega_c - \omega_m)t - \Delta\theta_m\right) + \cos\left((\omega_c + \omega_m)t + \Delta\theta_m\right)\right]\sin(\omega_c t) \tag{5.30}$$

$$V_B(t) \cong \frac{1}{4}V[\sin\left(\omega_m t + \Delta\theta_m\right) - \sin\left(\omega_m t + \Delta\theta_m\right)] \tag{5.31}$$

which is zero provided that the resonator has flat dispersion. The amplitude noise of the carrier is therefore a second order effect. If the frequency discriminator phase is badly detuned from the resonator center frequency, then amplitude noise may be important.

60Hz Spurs

A final technical noise source is magnetic pick-up of 60 Hz, which results in 60 Hz harmonics at the mixer output and may dominate the noise floor depending on the lock-in amplifier bandwidth.

5.5 Prototype Sensitivity

The chart summarizes the contributions of the various noise mechanisms to the system noise floor. The most important are the phase noise of the RF source and acoustic pickup from the modulation coils.

Noise Source	Transfer Function	Techniques
Oscillator Phase Noise	$\frac{P_{out}}{P_{PhaseNoise}} = \left(\frac{Q_L f_m}{f_0}\right)^2$	Reduce close-in phase noise or use carrier suppression design
Piezo Driver Noise	$\left\|\frac{V_{out}}{V_{piezo}}\right\| = V_{RF}\frac{Q_L K}{f_0}$	Driver output filter
Receiver Noise Figure	*-171 dBm/Hz @ 3dB NF*	Fundamental
Acoustics	$\Delta V_M \cong \frac{1}{2} V_{RF} \cdot \frac{Q_L}{f_0} \cdot \frac{1}{2}\frac{\Delta g}{g} f_0$	Re-Design Resonator

BIBLIOGRAPHY, CHAPTER 5

[1] F. L. Walls, "Suppressed Carrier Based PM and AM Noise Measurement Techniques," *Proc. IEEE International Frequency Control Symposium*, pp. 485-492, 1997.

[2] E. S. Ferre-Pikal, M. C. Delgado Aramburo, F. L. Walls, K. M. Lakin, "1/f Frequency Noise of 2-GHz High-Q Thin-Film Sapphire Resonators," *IEEE Trans. on Ultrasoonics, Ferroelectrics, and Frequency Control*, vol. 48, no. 2, pp. 506-510, March 2001.

[3] E. N. Ivanov, M. E. Tobar and R. A Woode, "Advanced Phase Noise Suppression Technique for Next Generation of Ultra-Low Noise Microwave Oscillators," *Proc. IEEE International Frequency Control Symposium*, pp. 314-320, 1995.

[4] D. Halford, A. E. Wainwright, and J. A. Barnes, "Flicker Noise of Phase in RF Amplifiers and Frequency Multipliers: Characterization, Cause and Cure," *Proc. IEEE Frequency Control Symposium*, pp. 340-341, 1968.